Thin-Walled Structures 171 (2022) 108657

Contents lists available at ScienceDirect

Thin-Walled Structures

journal homepage: www.elsevier.com/locate/tws

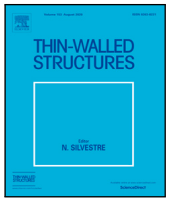

Full length article

Elastic shear buckling coefficients for diagonally stiffened webs

J.P. Martins *, H.S. Cardoso

University of Coimbra, ISISE, Department of Civil Engineering, Coimbra, Portugal

ARTICLE INFO

Keywords:
Shear buckling
Steel-plated structures
Diagonal stiffeners

ABSTRACT

In this paper, the characterisation of the elastic shear buckling behaviour of simply supported plates diagonally stiffened excluding the influence of direct stresses is made. Two broad numerical parametric studies consisting of linear buckling analysis by the finite element method are performed, covering the entire practical range of critical parameters like the aspect ratio and the stiffener's mechanical properties. In the first parametric study, attention is given to the influence of each parameter in the elastic critical shear stress. For that reason, a beam FE is chosen to model the stiffener, allowing the variation of each parameter individually. As it is systematically disregarded in previous studies, particular attention is given to the effect of the stiffener's torsional rigidity. The numerical models used in the second parametric study consist of full-shell FE, and the results are used to perform regression analysis that ultimately allowed to proposed two mathematical models for the analytical calculation of the elastic shear buckling coefficient: for open stiffeners over the compression diagonal and for closed cross-section stiffeners over the compression diagonal. The proposed mathematical models present excellent accuracy.

1. Introduction

The main driving force behind the design of steel I-girders is the maximisation of its resistance to direct stresses. For this reason, I-girders usually present thick flanges 'connected' by thin webs. However, the final design of some segments of continuous plate girders may be governed by other loading situations: for example, segments near internal supports where the highest hogging bending moment interacts with the highest shear force. In fact, in this situation, the final dimensions of the plate girders are the outcome of the design to direct stresses (mainly at the flanges), shear stresses at the web, and the interaction of direct stresses with shear stresses. In what concerns the shear stresses specifically, the collapse mode is associated with the shear buckling phenomena where the buckling of the web occurs due to the presence of a diagonal compression field arising over the compressive principal stress direction. For that reason, the thickness of the web governs the shear resistance of the plate girder. To cope with high shear forces leading to unreasonable thick webs, stiffening the web is the most appropriate solution to keep an economical design. Classical stiffening options are transverse and longitudinal stiffeners: the former helps control shear buckling by reducing the web panel's length, decreasing its slenderness, while the latter lessens the effects of shear buckling by providing an additional second moment of area. The third option to stiff the web consists of adding a diagonal stiffener between transverse stiffeners. This option has been disregarded in practice, mainly due to the lack of an official standardised method, and in research where it has received considerably less attention when compared to the 'classical' stiffening solutions.

The present paper explores the effect of considering diagonal stiffening in the elastic shear buckling behaviour of simply supported thin steel web plates under pure shear. This is performed by putting the stiffener's relative flexural and torsional stiffness and the panel's aspect ratio into evidence (where a is the length of the plate, b is the width of the plate, and $\alpha = a/b$ is called the aspect ratio of the plate).

2. Literature review

2.1. Unstiffened rectangular plates under shear stresses

In 1891 [1], Bryan studied the buckling behaviour of simply supported rectangular plates under uniaxial compression. Since then, the stability behaviour of flat plates has been the focus of many authors' work. In the field of plates under pure shear stresses, using the energy method, Timoshenko, in 1915 [2], was the first to give a solution to the linear stability problem of an unstiffened rectangular plate under uniform shear stresses. Many authors followed Timoshenko's work and provided solutions for plates with varying aspect ratios and different support conditions; a complete survey of those works and a description for each contribution is given by Bleich [3] until 1952. Later works worthy of being referenced are those from Cook & Rockey [4] and Bulson [5]. From these works, the following simplified solutions to

* Correspondence to: Civil Engineering Department, University of Coimbra, R. Luís Reis Santos - Pólo II, Pinhal de Marrocos, 3030-290 Coimbra, Portugal.
E-mail address: jpmartins@uc.pt (J.P. Martins).

https://doi.org/10.1016/j.tws.2021.108657
Received 26 May 2021; Received in revised form 29 October 2021; Accepted 3 November 2021
Available online xxxx
0263-8231/

compute the elastic critical stress (see Eq. (1)) are highlighted (where k_τ is the elastic shear buckling coefficient and α is the plate's aspect ratio) (see Eqs. (1)–(5))

$$\tau_{cr} = k_\tau \cdot \frac{\pi^2 \cdot E}{12\left(1-\nu^2\right)} \cdot \left(\frac{t}{b}\right)^2 \tag{1}$$

$$k_\tau = \begin{cases} 4 + \dfrac{5.34}{\alpha^2} & for\ \alpha \le 1 \\ 5.34 + \dfrac{4}{\alpha^2} & for\ \alpha > 1 \end{cases} \quad \text{For simply supported unstiffened rectangular plates in all edges} \tag{2}$$

$$k_\tau = \begin{cases} 5.6 + \dfrac{8.98}{\alpha^2} & for\ \alpha \le 1 \\ 8.98 + \dfrac{5.6}{\alpha^2} & for\ \alpha > 1 \end{cases} \quad \text{For unstiffened rectangular plates clamped in all edges} \tag{3}$$

$$k_\tau = \begin{cases} 5.61 - 1.99\alpha + \dfrac{8.98}{\alpha^2} & for\ \alpha \le 1 \\ 8.98 + \dfrac{5.61}{\alpha^2} - \dfrac{1.99}{\alpha^3} & for\ \alpha > 1 \end{cases} \quad \text{For unstiffened rectangular plates clamped on two opposite sides and simply supported on the other two (long edges clamped)} \tag{4}$$

$$k_\tau = \begin{cases} \dfrac{5.34}{\alpha^2} + \dfrac{2.31}{\alpha} - 3.44 + 8.39\alpha & for\ \alpha \le 1 \\ 5.34 + \dfrac{2.31}{\alpha} - \dfrac{3.44}{\alpha^2} + \dfrac{8.39}{\alpha^3} & for\ \alpha > 1 \end{cases} \quad \text{For unstiffened rectangular plates clamped on two opposite sides and simply supported on the other two (short edges clamped)} \tag{5}$$

2.2. Stiffened rectangular plates under shear stresses

Concerning longitudinally stiffened plates under shear, the work of Crate & Lo [6] is a pioneer one giving the 'exact' solution for the elastic critical stress of long web panels with one centric longitudinal stiffener. The mathematical solution is given function to the out-of-the-web bending relative flexural rigidity γ, defined as the ratio $(E{\cdot}I_s)/(h_w{\cdot}D)$. D is the plate's flexural stiffness ($D = E{\cdot}\,t_w{}^3/(12\cdot(1-\nu^2))$), I_s is the second moment of area of the stiffener alone in respect to the middle plane of the web panel and t_w is the thickness of the web panel. Höglund [7] proposed expression (6) to approximate these 'exact' solutions.

$$k_\tau = 5.34 + 1.36\sqrt[3]{\gamma} \tag{6}$$

It is worth mentioning that the solutions given by Crate & Lo and, consequently, the expression proposed by Höglund is valid for long plates where the longitudinal edges are simply supported. For shorter plates (*i.e.,* when transverse rigid stiffeners are closely spaced), Höglund [7] and Beg [8], respectively, proposed the following expressions through curve fitting numerical results obtained previously in [9]:

$$k_\tau = 5.34 + \frac{4}{\alpha^2} + \frac{3.45\gamma^{\frac{3}{4}}}{\alpha^2} \tag{7}$$

$$k_\tau = 4.1 + \frac{6.3 + 0.05\gamma}{\alpha^2} + 1.44\sqrt[3]{\gamma} \tag{8}$$

According to [8], Beg's equation is more accurate for stiffened plates with 1 or 2 stiffeners and $\alpha < 3$; for any other case (more than three stiffeners; and 1 or 2 stiffeners with $\alpha > 3$) Höglund's expression presents better results provided it is limited inferiorly by Eq. (6).

These expressions are the basis of the design expressions present in some standards, namely, Eqs. (9) and (10), given in prEN1993-1-5:2020 [10] to compute the elastic critical shear stress of longitudinally stiffened steel web panels. These expressions are obtained by reducing the stiffener's second moment of area in expressions (7) and (8) by 1/3. The justification for this is given in [7] and in [8]. It relates to the fact that stiffened plates show lower post-buckling strength reserve and, to keep using the same shear resistance reduction curve as for unstiffened plates (in light of the ease-of-use of standards), the second moment of area must be reduced. This justification is mainly valid for girders with heavy flanges, where its contribution to shear resistance is overestimated [11]. Additionally, in the case of closed cross-section stiffeners, it has been shown that the 1/3 reduction is not necessary [11–16] (mainly because expressions (9) and (10) do not consider the beneficial effect provided by the torsional stiffness; therefore a correction coefficient of $\beta_s = 3$ is included). Finally, according to the prEN1993-1-5:2020 [10], the definition of the cross-section of the stiffener includes adjacent parts of the web plate (see Fig. 1(a) for open cross-section and Fig. 1(b) for closed cross-section stiffeners).

$$k_\tau = \begin{cases} 4 + \dfrac{5.34}{\alpha^2} + \max\left\{ \dfrac{9}{\alpha^2}\sqrt[4]{\left(\dfrac{\beta_s \cdot I_s}{h_w \cdot t_w^3}\right)^3}\,; 2.1\sqrt[3]{\dfrac{\beta_s \cdot I_s}{h_w \cdot t_w^3}} \right\} & for\ \alpha \le 1 \\ 5.34 + \dfrac{4}{\alpha^2} + \max\left\{ \dfrac{9}{\alpha^2}\sqrt[4]{\left(\dfrac{\beta_s \cdot I_s}{h_w \cdot t_w^3}\right)^3}\,; 2.1\sqrt[3]{\dfrac{\beta_s \cdot I_s}{h_w \cdot t_w^3}} \right\} & for\ \alpha > 1 \end{cases} \tag{9}$$

$$k_\tau = 4.1 + \frac{6.3 + 0.18\frac{\beta_s \cdot I_s}{h_w \cdot t_w^3}}{\alpha^2} + 2.2\sqrt[3]{\frac{\beta_s \cdot I_s}{h_w \cdot t_w^3}} \tag{10}$$

Concerning diagonally stiffened plates, Dubas & Gehri [17] indicate fixed values for the elastic critical buckling factor for simply supported square web panels depending on the direction of the stiffener: $k_\tau = 30$ over the compression diagonal and $k_\tau = 11.4$ over the tension diagonal. Within the scope of diagonally stiffened plates, Dubas & Gehri also give an (incomplete) list of contributions up to 1984. Recently, Yuan et al. [18] provided a complete list of contributions, where the work of Yonezawa et al. [19] is highlighted as the authors provide with formulae to compute the elastic critical shear stress of simply supported web panels stiffened over the compression and tension diagonal (see Eqs. (11)–(14))

$$k_\tau = 11.9 + \frac{10.1}{\alpha} + \frac{10.9}{\alpha^2} \quad \text{For simply supported rectangular plates in all edges stiffened over the compression diagonal} \tag{11}$$

$$k_\tau = 14.7 + \frac{11.5}{\alpha} + \frac{15.8}{\alpha^2} \quad \text{For rectangular plates clamped in all edges stiffened over the compression diagonal} \tag{12}$$

$$k_\tau = 17.2 - \frac{22.5}{\alpha} + \frac{16.7}{\alpha^2} \quad \text{For simply supported rectangular plates in all edges stiffened over the tension diagonal} \tag{13}$$

$$k_\tau = 24.7 - \frac{32.4}{\alpha} + \frac{25}{\alpha^2} \quad \text{For rectangular plates clamped in all edges stiffened over the tension diagonal} \tag{14}$$

Nevertheless, the values proposed by Dubas & Gehri and the expressions by Yonezawa et al. present obvious limitations for practical applications, and none of the authors provide a way to include the relative flexural or torsional stiffness of the stiffener.

Yuan et al. [18] proposed a set of expressions suitable for stainless steel web panels stiffened over the compression diagonal and framed by upper and lower flanges and vertical stiffeners (*i.e.,* the edge's level of rotational restraint lies between the simply supported and rotationally fixed assumptions). From a regression analysis using numerically obtained results, the authors proposed expression (15). The main advancement of this expression is that it includes the effect of the stiffener's relative flexural stiffness (where the calculation of the stiffener's second moment of area includes adjacent parts of the web plate equal to $11\cdot\varepsilon\cdot t$ and done about the middle plane of the web

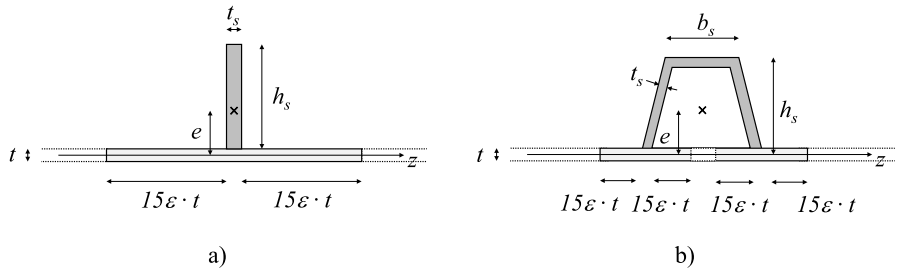

Fig. 1. Definition of stiffener's geometry for design purposes acc. to prEN1993-1-5:2020 [10].

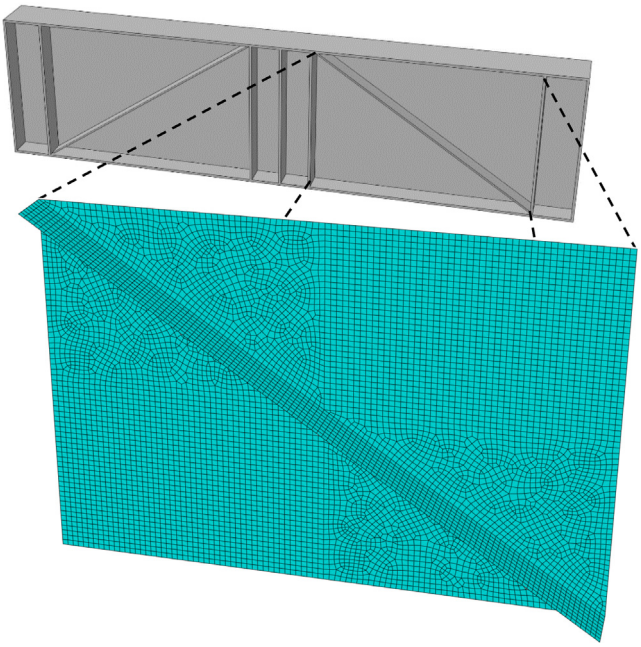

Fig. 2. Representation of the mesh for a web panel characterised by $\alpha = 1.5$ where the stiffener is over the compressed diagonal.

plate).

$$k_\tau = \begin{cases} \left(\frac{24.2}{\alpha} - 2\right) \cdot \sqrt[3]{\frac{I_s}{h_w \cdot t_w^3}} + \frac{6.57}{\alpha^2} + 4.92 \; for \; \frac{I_s}{h_w \cdot t_w^3} < 1 \wedge \alpha < 1 \\ \left(\frac{24.2}{\alpha} - 2\right) \cdot \sqrt[3]{\frac{I_s}{h_w \cdot t_w^3}} + \frac{4.92}{\alpha^2} + 6.57 \; for \; \frac{I_s}{h_w \cdot t_w^3} < 1 \wedge \alpha \geq 1 \\ \left(\frac{9}{\alpha} - 2\right) \cdot \sqrt[3]{\frac{I_s}{h_w \cdot t_w^3}} + \frac{6.57}{\alpha^2} + \frac{15.2}{\alpha} + 4.92 \; for \; \frac{I_s}{h_w \cdot t_w^3} \geq 1 \wedge \alpha < 1 \\ \left(\frac{9}{\alpha} - 2\right) \cdot \sqrt[3]{\frac{I_s}{h_w \cdot t_w^3}} + \frac{4.92}{\alpha^2} + \frac{15.2}{\alpha} + 6.57 \; for \; \frac{I_s}{h_w \cdot t_w^3} \geq 1 \wedge \alpha \geq 1 \end{cases} \quad (15)$$

The expression proposed by Yuan et al. represents a non-negligible improvement. However, it still disregards the significant effects of the stiffener's torsional rigidity, which is non-negligible in closed cross-section stiffeners. Furthermore, it is not suitable for simply supported web panels (common assumption used in standardised design methods).

As far as the authors' knowledge reaches, the most up-to-date work is from Glassman et al. [20]. The authors explore the effectiveness of diagonal stiffening concerning buckling and post-buckling strength reserve for ambient and elevated temperatures.

3. Numerical model

3.1. General considerations

All numerical simulations consisted of linear buckling analyses (LBA) and were performed using ABAQUS FEA software [21]. All models analysed in this study are diagonally stiffened flat thin steel ($E = 210\,000$ N/mm^2) plates under pure shear. Therefore, as all plates have two dimensions much larger than the thickness, a shell FE is chosen (see more details in 3.2). Two models were utilised: shell FE (Section 5) and shell FE coupled with beam FE for the stiffener (Section 4).

To have complete control of the mechanical properties avoiding at the same time material duplication (see full description in 3.3), beam FE model the diagonal stiffener. In this way, it is possible, for instance, to study the effect of increasing the flexural stiffness of the stiffener without increasing its relative torsional stiffness. On the other hand, real engineering applications commonly use the stiffener welded only on one side of the panel. Consequently, an eccentricity arises whose effect is more accurately covered by shell FE models. One final remark should be made concerning the different behaviour of the stiffeners depending on how it is modelled: where shell FE models the stiffener, local buckling modes associated with the stiffener may appear, introducing a bias in the numerical results; to avoid this bias, all models are post-processed by a python script which identifies those which present a first buckling mode including local deformations on the stiffener excluding them from the analysis made in Section 5.

3.2. Mesh

As already highlighted, as the numerical models under analysis represent thin web panels with two dimensions much larger than the thickness, it is acceptable to use a 2D finite element. In this case, the models use a general-purpose S4R shell element. This element has a finite-membrane-strain formulation with four nodes with 6 DOF each, making it suitable for structural problems where in-plane compression and bending appear together with out-of-plane deformations. The main goal of mesh refinement is to obtain converged results. Thus, the more refined the mesh, the better the numerical result is, but the more time is spent during the analysis. An ideal mesh leads to converged numerical results while keeping the run-time of the numerical analysis under an 'acceptable' timeframe. After a mesh convergence study (on the elastic buckling load) for all models, a mesh consisting of 65 FE over the plate's depth led to accurate (i.e., converged) results in a satisfactory amount of time. As it will be further detailed, the stiffener was modelled by beam FE, more specifically B33 beam FE coupled with shell FE. This type of beam FE is 2-noded with a cubic interpolation scheme indicating that it is accurate for distributed loading along the beam. They allow axial, bending, and torsional deformation. Fig. 2 shows the

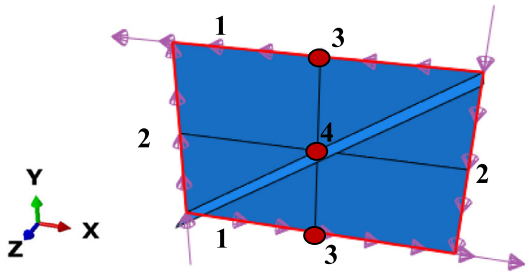

Degrees of Freedom	Region 1	2	3	4
u_x			X	
u_y				X
u_z	X	X		
θ_x		X		
θ_y	X			
θ_z	X	X		

Fig. 3. Representation of model partitions, loading application and boundary conditions.

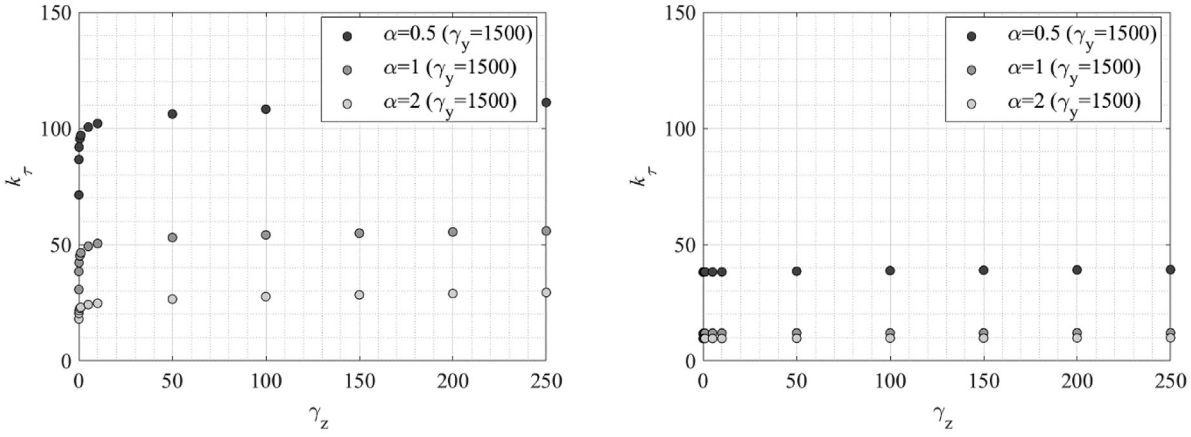

Fig. 4. Effect of γ_z in the elastic critical shear buckling coefficients: *(a)* stiffener over the compression diagonal and *(b)* stiffener over the tension diagonal.

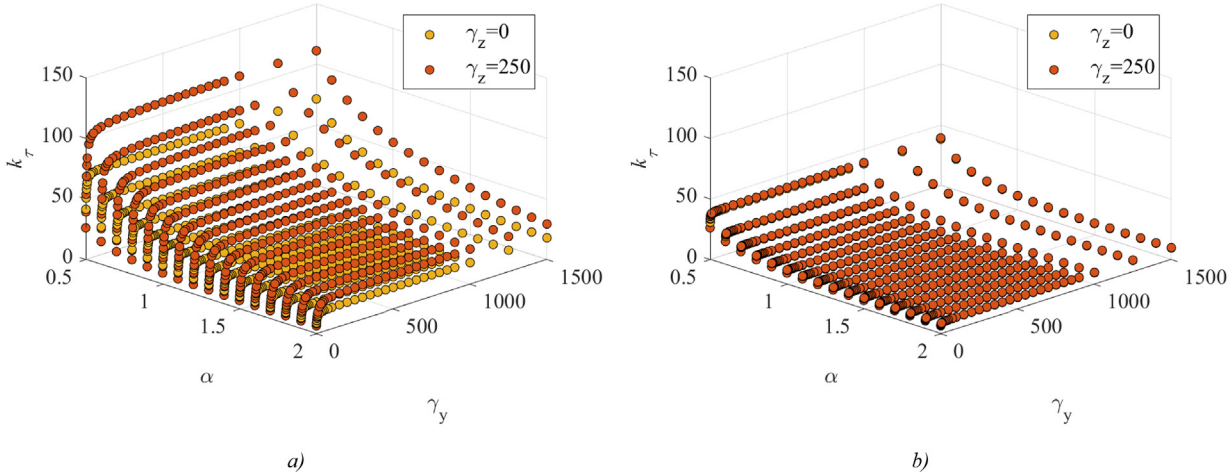

Fig. 5. 3D plot of k_τ results for *(a)* $\gamma_z = 0$ and $\gamma_z = 250$ and stiffener over the compression diagonal and *(b)* $\gamma_z = 0$ and $\gamma_z = 250$ and stiffener over the tension diagonal.

resulting mesh for a web panel characterised by $\alpha = 1.5$ and stiffener over the compressed diagonal.

3.3. Loading and support conditions

All numerical models of the web panels are under pure shear modelled by line loads applied over the plate's edges (Fig. 3). Regarding the modelling of the stiffener, it consists of a beam FE coupled with shell FE along the diagonal of the plate. Because the stiffener bends along the diagonal of the plate, its out-of-plane displacements are not constant, and, therefore, a rigid motion constraint over the entire length of the stiffener cannot be employed. Thus, beam FE endowed with the stiffener's mechanical properties are coupled with the shell FE and the

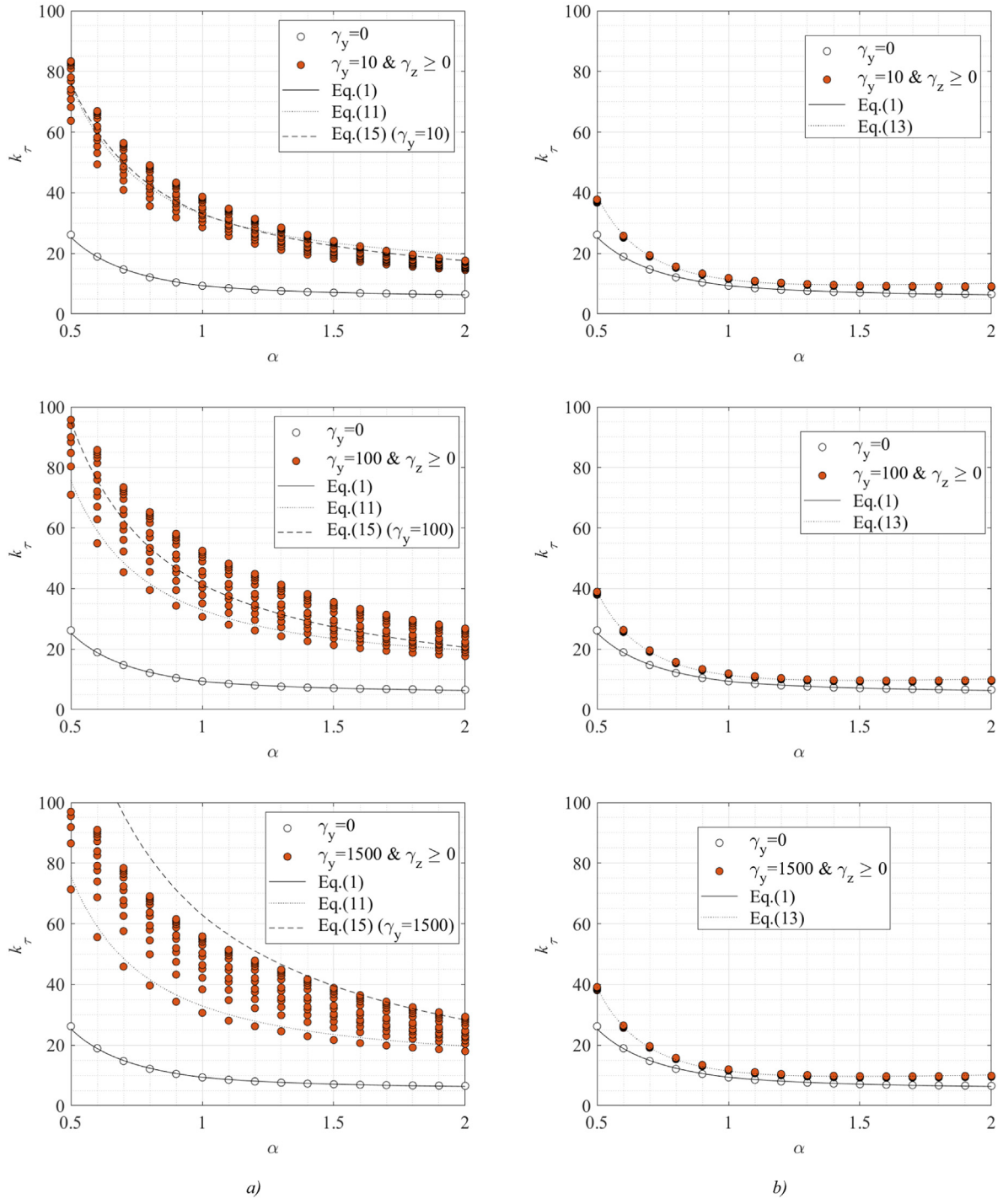

Fig. 6. 2D plot of α-k_τ curves for the entire range of γ_z with *(a)* stiffener over the compression diagonal and *(b)* stiffener over the tension diagonal.

plate's diagonal (compression and tension) and at its middle plane. Finally, this way of modelling the stiffeners does not allow for the consideration of stiffeners with slender cross-sections, i.e., prone to local buckling, as the beam FE cannot capture the drop in the stiffness of the locally buckled stiffener.

4. Parametric study

4.1. Scope

Classically, in parametric studies involving simply supported unstiffened panels under pure shear, the aspect ratio range is limited to long panels ($\alpha \geq 1$) as the shear buckling coefficients for shorter panels may be obtained by using the values of a corresponding panel with aspect ratio $1/\alpha$ where the roles of the width and length are switched. However, in this study, the definition of a stiffener relative flexural stiffness uses the width of the plate, and it is not possible to switch over the roles of width and length. For this reason, the aspect ratio varies from 0.5 to 2 (with a step of 0.1) (in fact, the stiffening of the web along its compression diagonal only makes sense in regions where the shear force is high; this happens in regions near internal supports of continuous beams where values of the web plate aspect ratio are typically under 2).

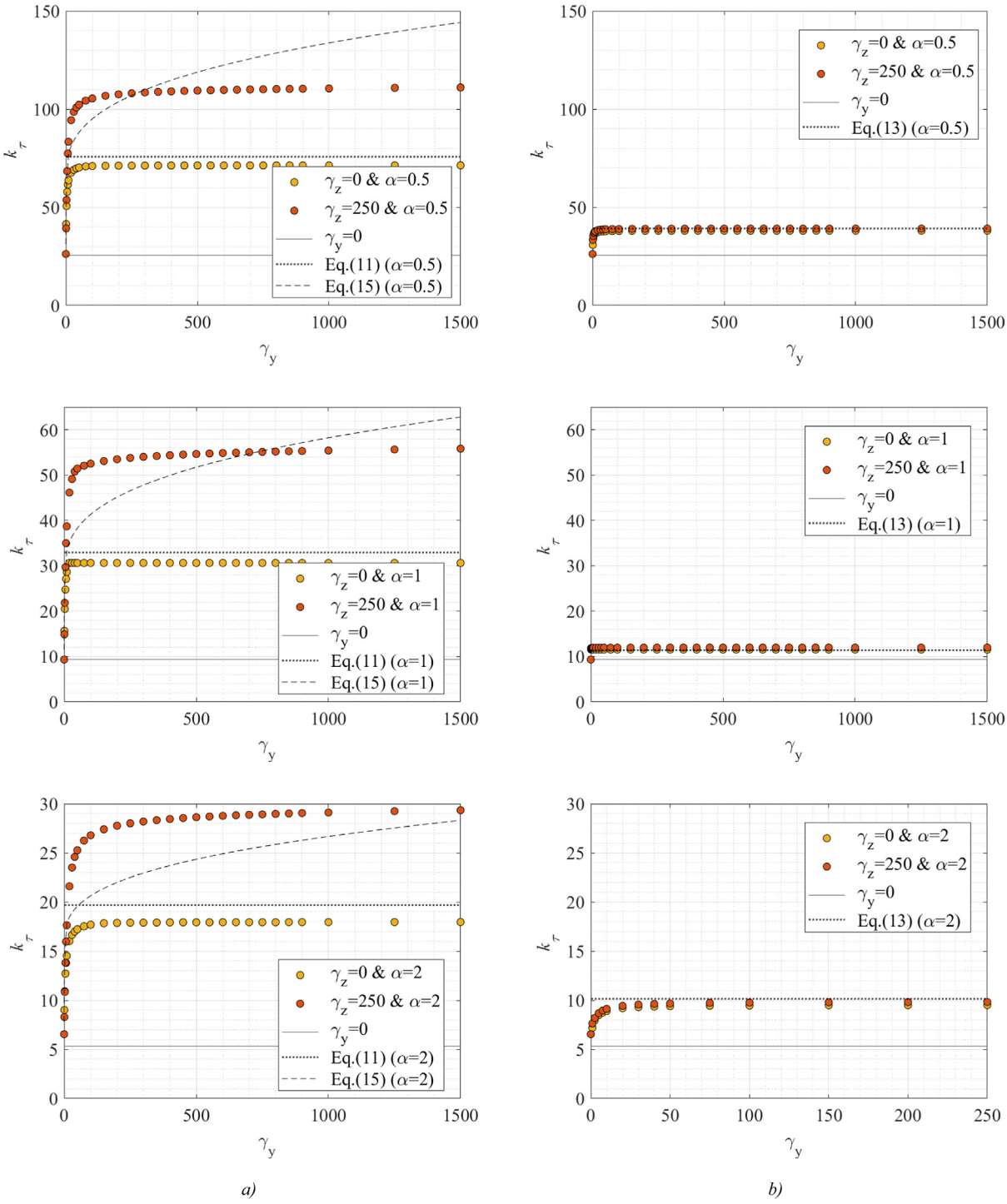

Fig. 7. 2D plot of γ_y-k_τ curves for *(a)* $\gamma_z = 0$ and $\gamma_z = 250$ and stiffener over the compression diagonal and *(b)* $\gamma_z = 0$ and $\gamma_z = 250$ and stiffener over the tension diagonal.

Concerning the stiffeners, the following mechanical properties are set as parameters: relative flexural rigidity around the strong axis ($I_{y,s}$ computed with reference to the middle plane of the web panel), see Eq. (16); relative flexural rigidity around the weak axis ($I_{z,s}$ computed with reference to the centre of mass of the stiffener alone), see Eq. (17); and relative torsional rigidity ($I_{T,s}$ computed with reference to the centre of mass of the stiffener alone), see Eq. (18).

$$\gamma_y = \frac{E \cdot I_{y,s}}{h_w \cdot D} \tag{16}$$

$$\gamma_z = \frac{E \cdot I_{z,s}}{h_w \cdot D} \tag{17}$$

$$\phi_x = \frac{G \cdot I_{T,s}}{h_w \cdot D} \tag{18}$$

Table 1 shows the practical range of the above-defined mechanical properties of stiffeners. This table results from a literature survey for open- and closed-section stiffeners. Due to the scarcity of examples found with stiffeners deployed diagonally over the web panel, the survey includes plates longitudinally stiffened. Furthermore, the presented values were recalculated assuming the geometric values of the stiffener

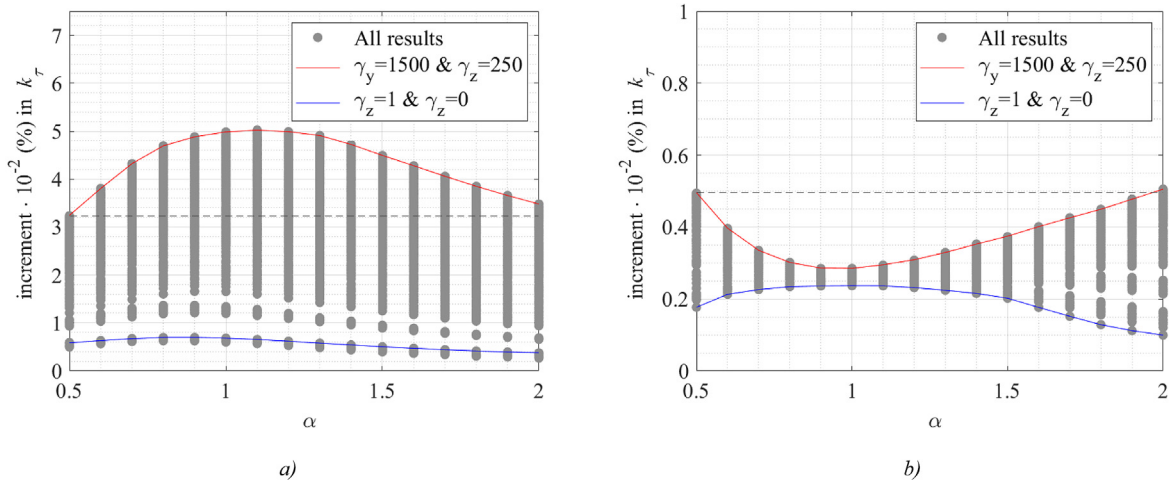

Fig. 8. Observed increment in the elastic critical shear buckling coefficients (effect of adding diagonal stiffener): *(a)* stiffener over the compression diagonal and *(b)* stiffener over the tension diagonal.

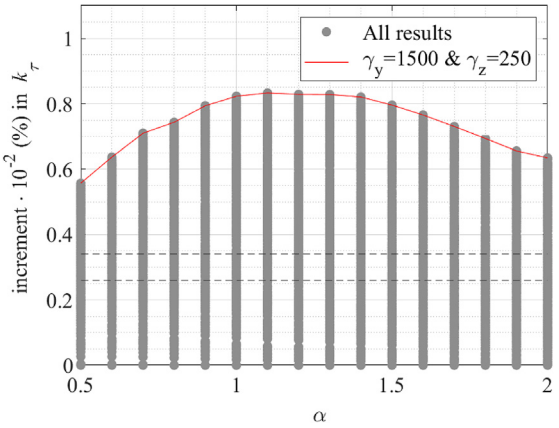

Fig. 9. Observed increment in the elastic critical shear buckling coefficients (isolated effect of stiffener's weak axis rigidity) when the stiffener is placed over the compression diagonal.

Table 1
Survey on the range of mechanical properties of the stiffeners.

Open-section stiffeners	γ_y	γ_z	ϕ_x
Dubas & Tschampeer [22]	308.9	0.3	0.475
Graciano & Lagerqvist [23]	129.8	0.1	0.196
Loaiza et al. [24]	57.8–61.4	0.022–0.073	0.034–0.107
Loaiza et al. [25]	12.6–2396.9	0.015–3.7	0.023–5.384
Markovic & Kovacevic [26]	29.8	0.4	0.559
Yonezawa et al. [19]	15.9	0.17	0.225
Yuan et al. [18]	15.5	0.1	0.077
Beg et al. [27]	85.3	0.19	0.28
Closed-section stiffeners	γ_y	γ_z	ϕ_x
Carretero & Lebet [28]	128.4–416.9	46.1–55.7	41.0–138.3
Kulhmann et al. [29]	95.2	48.2	42.7
Dubas & Tschampeer [22]	172	62.6	51.9
Graciano & Lagerqvist [23]	6.5–939.3	1.4–233.1	1.6–252.1
Loaiza et al. [24]	51.7–782.8	12.1–194.2	13.1–210.1
Pavlovic et al. [30]	26.6–146.5	13.2–41.3	10.8–39.5
Seitz [31]	324.1–679.3	78.7–221.7	85.4–194.4
Sinur & Beg [32]	105.3	75.5	58.1
Biscaya et al. [33]	108.1	60.3	51.2

alone and to the middle plane of the plate according to the above equations.

Table 2 defines the parametric range making use of the information given in Table 1. It comprises three sets of analyses, totalising

Table 2
Values of the relative mechanical properties of the stiffeners used in the parametric study.

Parameter	Range
Plate's aspect ratio, α	{0.5; 0.6 0.7; 0.8; 0.9; 1.0; 1.1; 1.2; 1.3; 1.4; 1.5; 1.6; 1.7; 1.8; 1.9; 2.0}
Stiffener's relative flexural rigidity around the strong axis, γ_y	{0; 1; 2.5; 5; 7.5; 10; 20; 30; 40; 50; 75; 100; 150; 200; 250; 300; 350; 400; 450; 500; 550; 600; 650; 700; 750; 800; 850; 900; 1000; 1250; 1500}
Stiffener's relative flexural rigidity around the weak axis, γ_z	{0; 0.01; 0.1; 0.5; 1; 5; 10; 50; 100; 150; 200; 250}
Stiffener's relative torsional rigidity, ϕ_x	{0; 0.01; 0.1; 0.5; 1; 5; 10; 50; 100; 150; 200; 250}

17 856 linear buckling analyses. These sets are defined as follows (see numerical results in Section 4.2):

- Set 1 = $\{\alpha\} \times \{\gamma_y\} \times \{\gamma_z\} \times \{\phi_x = 0\}$
- Set 2 = $\{\alpha\} \times \{\gamma_y\} \times \{\gamma_z = 0\} \times \{\phi_x\}$
- Set 3 = $\{\alpha\} \times \{\gamma_y\} \times \{\gamma_z = 250\} \times \{\phi_x\}$

4.2. Results and discussion

4.2.1. Preliminary remarks

This study comprises an extensive parametric range where elastic shear buckling coefficients for diagonally stiffened plates are calculated, varying the aspect ratio and three parameters related to the mechanical properties of the stiffener, making the problem a five-dimensional one. For that reason, it is not possible to simply display the results in 2D or 3D plots. The choice was made to separate each analysis into two: a first one plotting the numerical results against the aspect ratio, the stiffener's flexural rigidity around the strong axis, and the stiffener's flexural rigidity around the weak axis (where the stiffener's torsional rigidity is set to zero); and a second one plotting the numerical results against the aspect ratio, the stiffener's flexural rigidity around the strong axis, and the stiffener's torsional rigidity (where the stiffener's rigidity around the weak axis is set to its upper and lower bounds). Therefore, the parametric study assumes the panel's aspect ratio and the stiffener's flexural rigidity around the strong axis as critical parameters. In contrast, the effect of the remaining parameters is brought into evidence by allowing visualisation of upper and lower bounds.

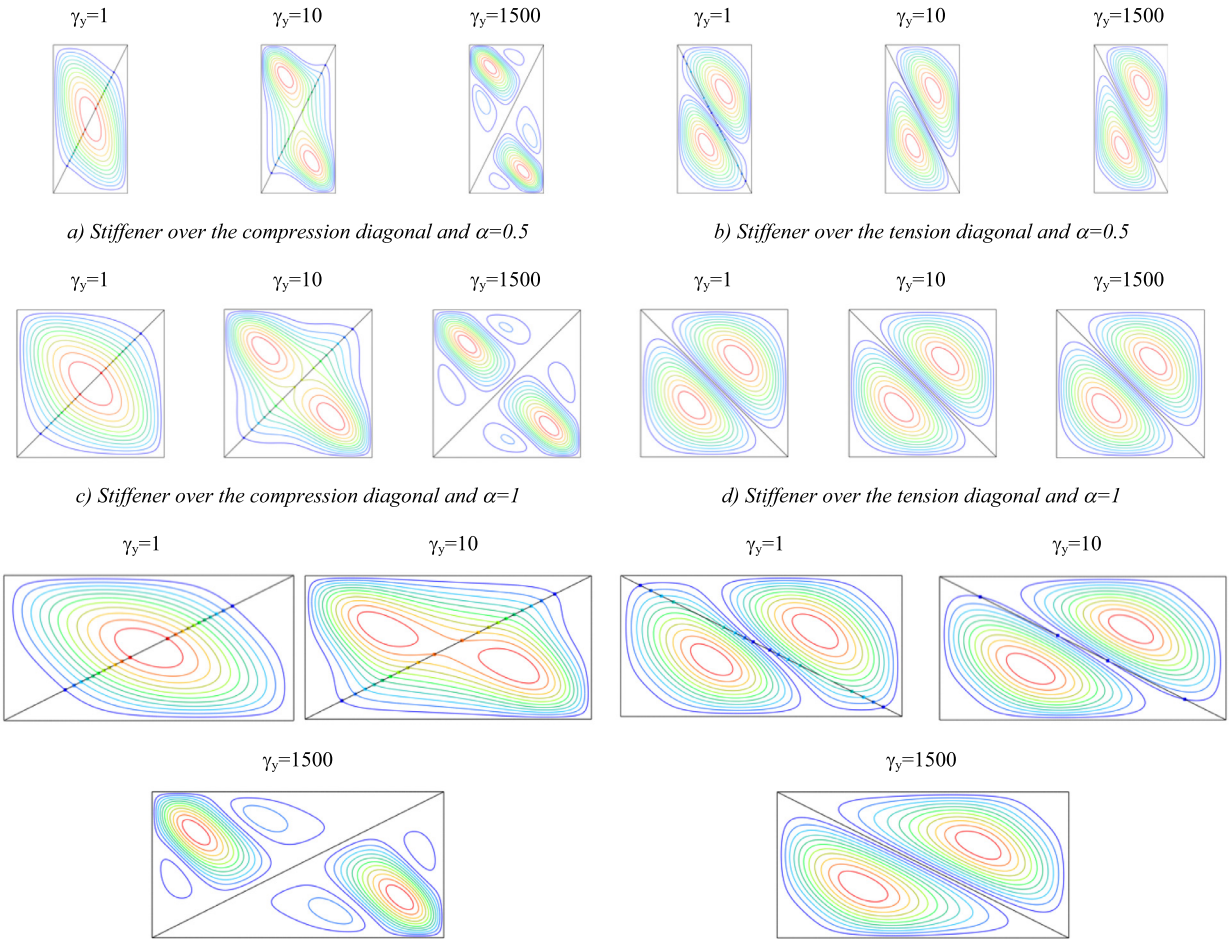

Fig. 10. 1st Eigenmodes observed for plates with several aspect ratios where the stiffener is characterised by γ_y = 1, 10 & 1500 and γ_z = 250.

As a general trend throughout the following sections, as expected and confirming what has already been concluded by other authors, placing the stiffener over the diagonal in compression returns consistently higher values of shear buckling coefficients when comparing the same analysis with the stiffener set over the tension diagonal.

4.2.2. Effect of the stiffener's flexural rigidity around the weak axis

Fig. 4 shows the evolution of the elastic shear buckling coefficient with increasing values of the stiffener's weak axis rigidity (and for fixed values of strong axis rigidity, γ_y = 1500). It is evident that only when the stiffener is placed over the compressed diagonal a tangible effect is obtained for the elastic shear buckling coefficients. This apparent trend is observable for other values of γ_y, as proven in the following paragraphs.

For a more general analysis, Fig. 5 plots the results for the elastic shear buckling coefficients against the aspect ratio and the stiffener's strong axis rigidity and the lowest and highest values of γ_z (0 and 250). The resulting plot is a lower and upper bound scatter containing all possible results for stiffeners (neglecting the torsional rigidity, $\phi_x \approx 0$).

To enable the reading of the information provided by Fig. 5, Figs. 6 and 7 give 2D plots: in Fig. 6, the α-k_τ curves are plotted considering γ_y = 0, γ_y = 10, γ_y = 100, and γ_y = 1500 for both cases of stiffener configuration (over the compression and tension diagonals); in Fig. 7 γ_y-k_τ curves are shown for α = 0.5, 1 and 2. As expected, an increasing value of the stiffener's flexural rigidity around the weak axis results in a non-negligible increment in the value of the shear buckling coefficients within the entire range of the aspect ratio. This trend is significantly stronger when the stiffener is over the compression diagonal.

Concerning the effect of adding a diagonal stiffener, the maximum increment obtained is 502% (for α = 1.1, γ_y = 1500 and γ_z = 250) when the stiffener is placed over the compression diagonal and 51% (for α = 2γ_y = 1500 and γ_z = 250) when placed over the tension diagonal (Fig. 8). By observing Fig. 8, it is possible to state that the effect of adding a diagonal stiffener is more pronounced for values of aspect ratio around 1.0 (square panels) when placed over the compression diagonal. On the other hand, when placed over the tension diagonal, this effect shifts to panels with a lower or higher aspect ratio. In both cases, the highest values of increment are seen for models where γ_y = 1500.

Placing the stiffener over the compression diagonal, and taking into consideration solely the effect of varying its weak axis rigidity (from γ_z = 0 to 250), the increment in the elastic critical shear stress is 83% (for α = 1.1, γ_y = 1500 and γ_z = 250) (Fig. 9). On the other hand, placing the stiffener over the tension diagonal has an almost negligible effect (~8%).

Fig. 10 shows the buckling modes of some of the tested models. Specifically, it presents the buckling modes of models with a low aspect ratio (α = 0.5), aspect ratio equal to 1, and high aspect ratio (α = 2) for values of γ_y equal to 1, 10, and 1500.

It is observed that, for stiffeners over the compression diagonal, nodal lines do not appear while the stiffener is weak. This mechanical behaviour occurs because the diagonal in compression is unstable by nature, and an effective stabilising effect provided by a stiffener is only attained when it is strong enough, i.e. when it possesses a

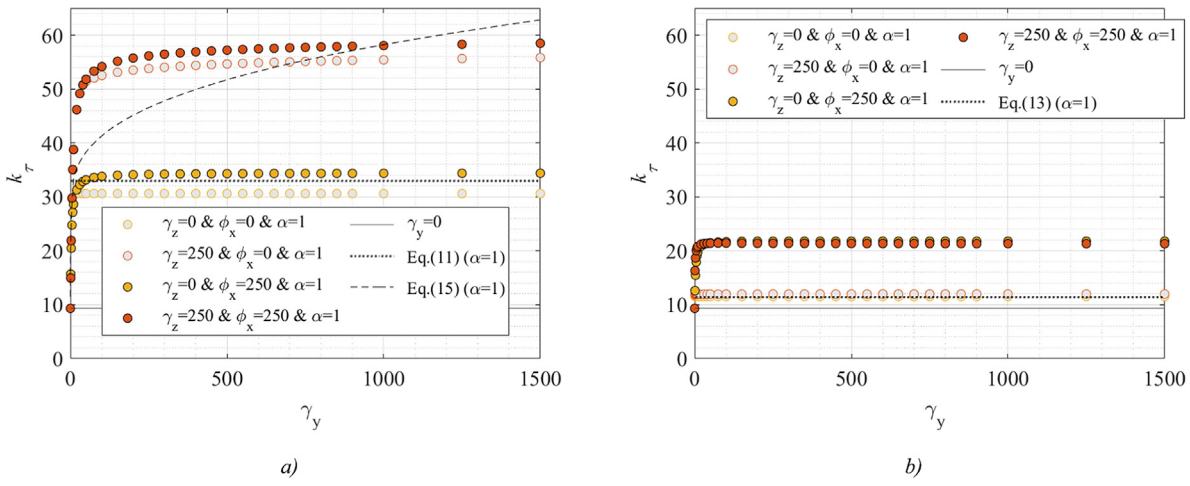

Fig. 11. 2D plot of γ_y-k_τ curves for: (a) γ_z = 0 and γ_z = 250 where φ_x = 0 and φ_x = 250 and stiffener over the compression diagonal and (b) γ_z = 0 and γ_z = 250 where φ_x = 0 and φ_x = 250 and stiffener over the tension diagonal.

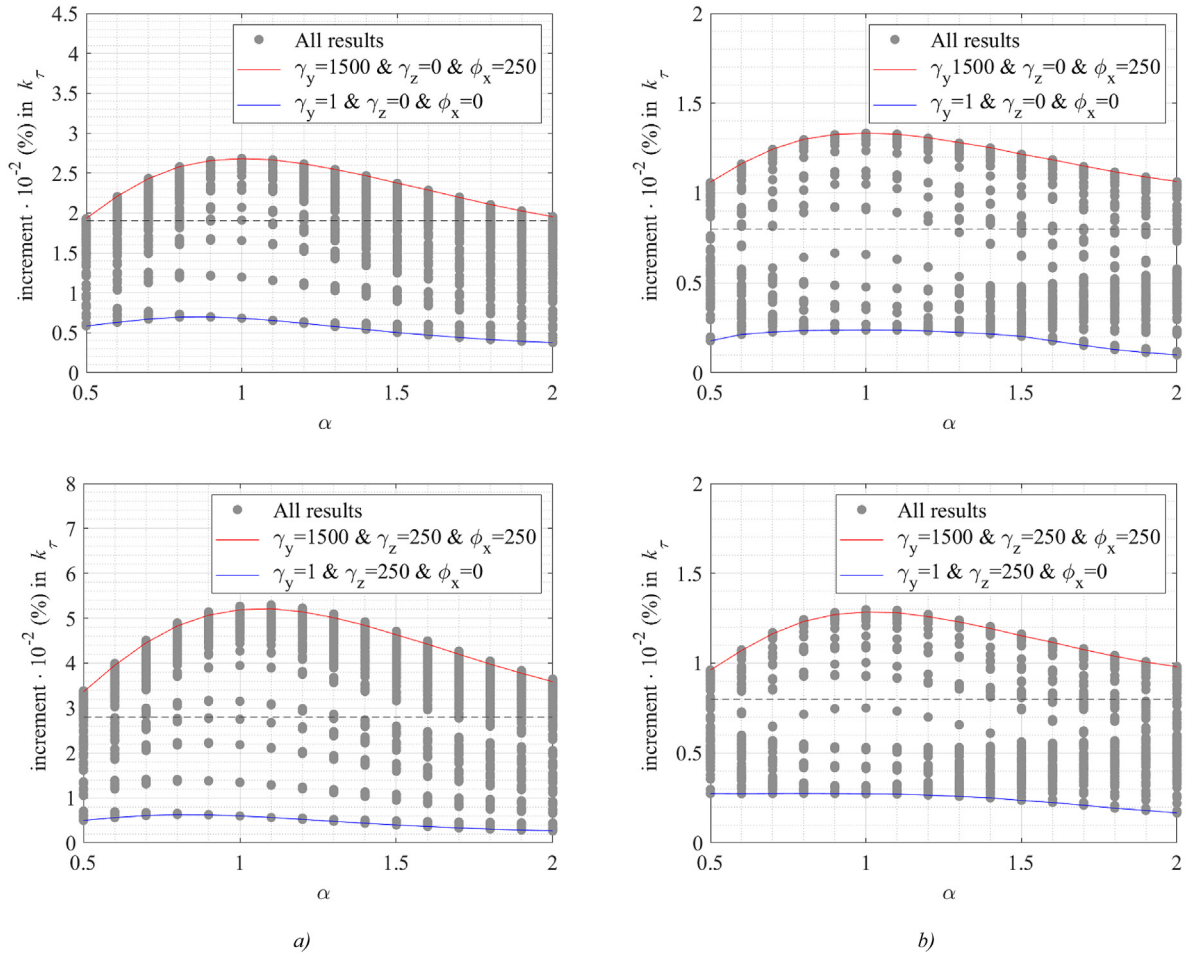

Fig. 12. Observed increment in the elastic critical shear buckling coefficients (effect of considering the stiffener's torsional rigidity): (a) γ_z = 0 and γ_z = 250 and stiffener over the compression diagonal and (b) γ_z = 0 and γ_z = 250 and stiffener over the tension diagonal.

sufficiently high critical stress to prevent the web from shear buckling. This stabilisation effect starts for values of γ_y around 10. On the other hand, the diagonal in tension tends to be stable by nature, and a nodal line appears even for very weak stiffeners. In this case, the effect of a strong stiffener is only shifting the position of the nodal line forcing it to be coincident with the stiffener itself. This effect is less pronounced for panels with α around one and absent for panels with α = 1, mechanically explaining the fact why the increment in Fig. 8(b) is higher for panels with α = 0.5 and α = 2 than for panels where α is close to 1. Moreover, as already mentioned in Section 4.1, had the panels been unstiffened and only those with α > 1 would be necessary to calculate the elastic shear buckling coefficient for the entire parametric range. The very similar buckling shapes of panels with α = 0.5 and α = 2 (see Fig. 10) make the corroboration of this

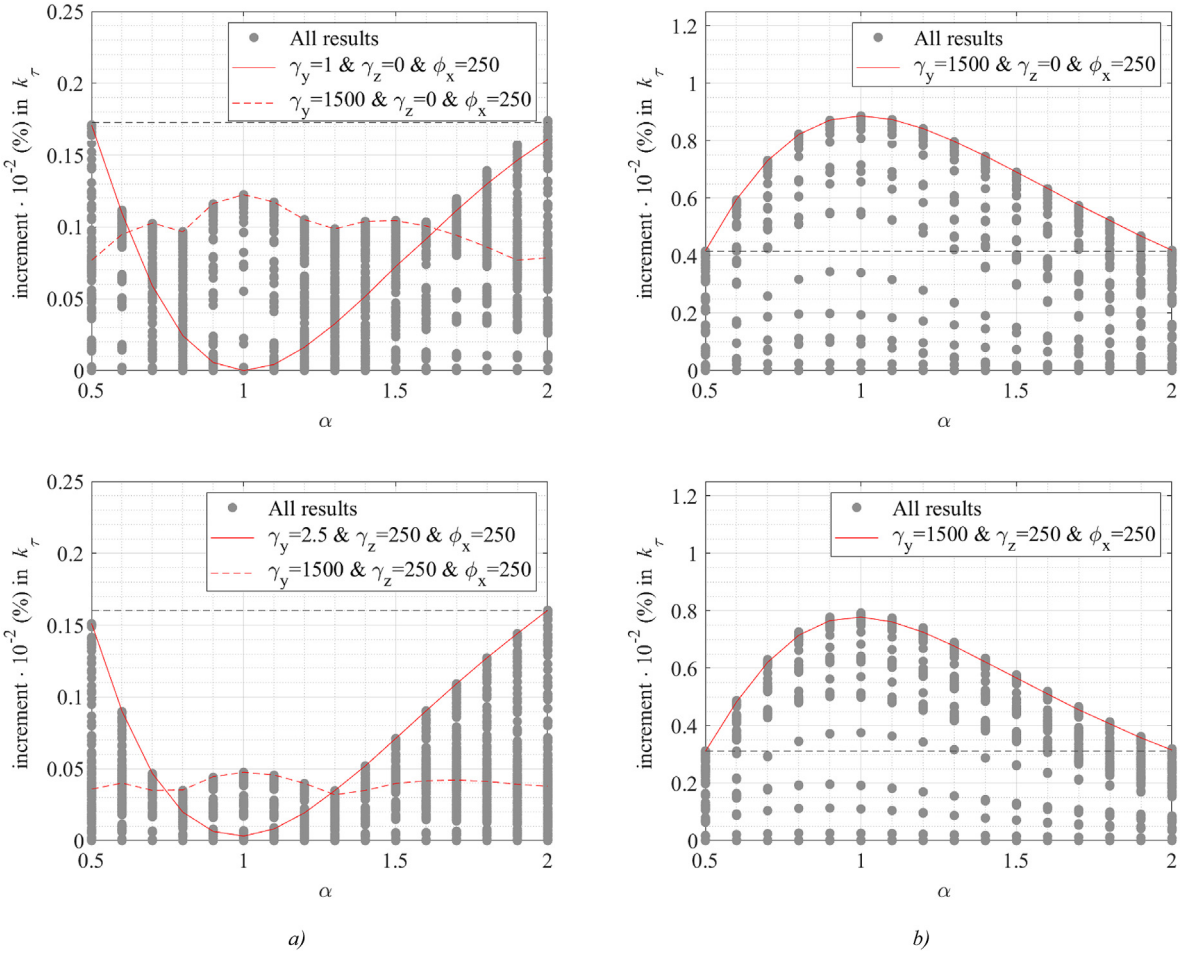

Fig. 13. Observed increment in the elastic critical shear buckling coefficients (isolated effect of stiffener's torsional rigidity): (a) $\gamma_z = 0$ and $\gamma_z = 250$ and stiffener over the compression diagonal and (b) $\gamma_z = 0$ and $\gamma_z = 250$ and stiffener over the tension diagonal.

statement. This is the reason why in Fig. 8, the increment for panels at both ends of the parametric range of aspect ratio is almost the same (conclusion highlighted by the black dashed line in Fig. 8(b)). On the other hand, placing the stiffener over the compression diagonal has the maximum increment for aspect ratios around 1 (Fig. 9(a)). The mechanical explanation for this fact is that 45º is the angle that maximises the force transferred to the stiffener.

4.2.3. Effect of the stiffener's torsional rigidity

The information provided throughout Figs. 4-10 is related to models neglecting the stiffener's torsional rigidity (it is intentionally set to zero in the beam FE properties). Nevertheless, the torsional rigidity is always present (even for stiffeners with open cross-sections, however small it may be). As an example, Fig. 11 shows the effect of considering the stiffener's torsional rigidity (considered with the highest value assumed in the parametric range, i.e., ($\varphi_x = 250$), in the shear buckling stress of a square panel. The stiffener's torsional stiffness increases with a non-negligible impact when the stiffener is placed over the compression or the tension diagonal, as shown in these charts.

Fig. 12 quantifies the impact that taking the stiffener's torsional rigidity into account has. It is seen an increment of 530% (for $\alpha = 1.1$, $\gamma_y = 1500$, $\gamma_z = 250$ and $\varphi_x = 250$) when the stiffener is placed over the compression diagonal and 130% ($\alpha = 1.0$–1.1 $\gamma_y = 30$–1500, $\gamma_z = 0$ & 250 and $\varphi_x = 100$–250) when placed over the tension diagonal.

Looking solely at the effect of varying the stiffener's torsional rigidity (from $\varphi_x = 0$ to 250), Fig. 13 shows an increment of 16%–17% when placed over the compression diagonal and 79%–89% over the tension diagonal.

5. Formulae for shear buckling coefficients

5.1. Preliminary remarks

In light of proposing formulae to calculate shear buckling coefficients of diagonally stiffened plates, it is reasonable to consider practical dimensions for the stiffeners. Furthermore, current engineering practice places the stiffeners over one side of the web plate (unsymmetric layout). In opposition to longitudinally stiffened plates, this creates an eccentricity of the shear loading in respect to the centre of mass of the structural model. Consequently, a destabilising bending moment arises, leading to a lower critical shear load when compared to a model where the stiffener (equal second moment of area in respect to the plate's middle surface) is symmetrically placed. Fig. 14 illustrates this phenomenon.

Therefore, two additional sets of analyses consisting of shell FE models were defined (8618 analyses for open stiffeners over compression diagonal (set 4) and 10 061 analyses for closed cross-section stiffeners over the compression diagonal (set 5). These models consider the stiffener placed at one side (unsymmetric layout). The ranges of these two additional sets are plotted in Fig. 15 (for all aspect ratios given in Table 2) and compared to the values retrieved from the survey (Table 1). The proposed models in Section 5 were fitted using the data of these sets.

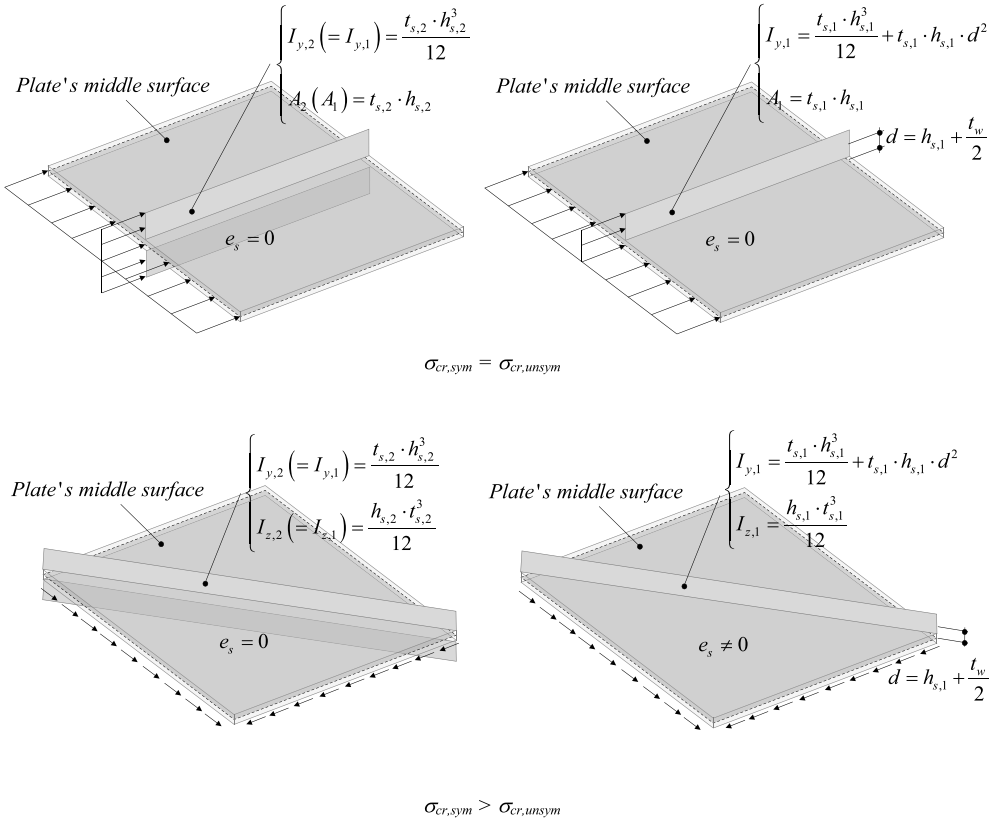

Fig. 14. Symmetric *vs.* unsymmetric layout of stiffeners (where e_s is the eccentricity between the mass centre and stress resultant).

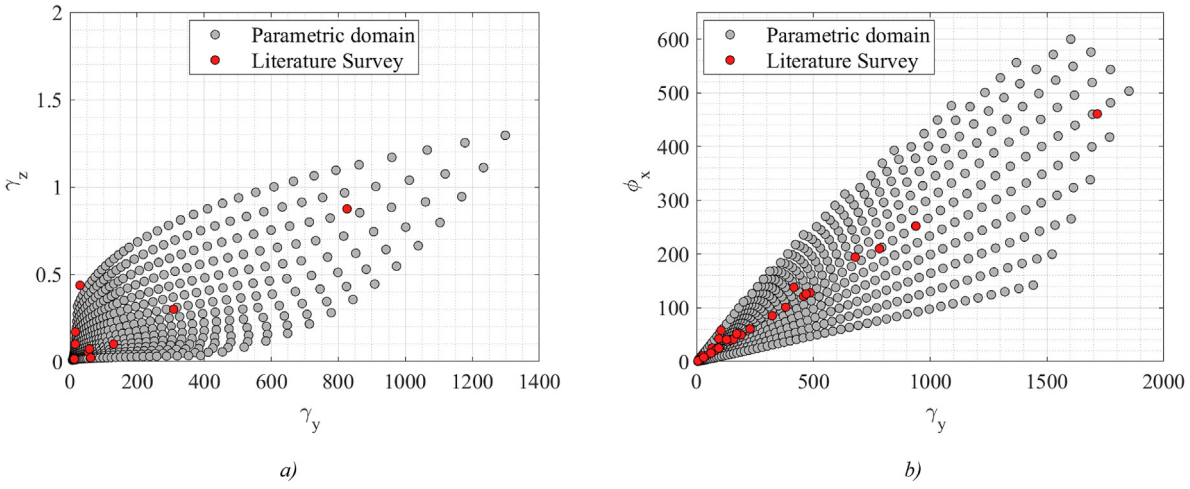

Fig. 15. Parametric domains of *(a)* set 4 (open stiffeners) and *(b)* set 5 (closed cross-section stiffeners).

5.2. Proposed formulae for simply supported panels

Looking at square panels where the stiffeners are effective (i.e., high values of γ_y), the values obtained when neglecting γ_z are $k_{\tau,c,FEM}$ = 32.56 and $k_{\tau,t,FEM}$ = 11.6 which are very close to those proposed in [17]. However, within the remaining parametric scope, as the values presented in [17] are too far apart from the numerical results, they are not appropriate for design purposes. Additionally, looking at Figs. 6(a), 7(a), and 11(a), it is possible to conclude that for simply supported panels stiffened over the compression diagonal, current formulae present non-negligible deviations from the numerical results. Eq. (11) by Yonezawa et al. [19] is only able to accurately capture the elastic critical stress in models where the relative flexural rigidity around the weak axis is ignored ($\gamma_z = 0$). In Yuan et al. [18] curve, it is acknowledged that the primary source of deviations comes from the fact that the level of restraint assumed for the edges lies between the simply supported and the rotationally fixed assumptions. In contrast, the results obtained from the numerical analyses are based on a simply supported assumption (as previously described).

On the other hand, panels stiffened over the tension diagonal Eq. (13) proposed by Yonezawa et al. [19] give accurate results when the stiffener's torsional stiffness is low, as it is patent in Figs. 6(b) and 7(b). However, analysing Fig. 11(b), it is possible to conclude that adding torsional stiffness to the stiffener produces a non-negligible

Table 3
Statistical parameters of the proposed formulae.

	No. of analysis	R^2	Mean	Co.V. (%)	Max. Abs. error (%)
Open stiffeners over the compression diagonal	8618	0.9994	0.9996	1.12	6.64
Closed stiffeners over the compression diagonal	10 063	0.9990	1.0004	1.51	9.37

effect on the elastic critical stress. Therefore, the need for improved formulae lies only on the side of panels stiffened over the compression diagonal and panels stiffened over the tension diagonal where the stiffener possesses non-negligible torsional stiffness, *i.e.,* closed cross-section stiffeners. However, as previously concluded, placing the stiffener over the tension diagonal is considerably less effective than putting it over the compression diagonal, reason why no formula is proposed for this case.

After testing several mathematical models, the one which returned the best results and, therefore, used to fit the data generated in sets 4 and 5 is defined by Eq. (19). Based on previous authors work, and on the results from Section 4, it was decided to perform the fitting for four subsets: for $\alpha < 1 \wedge \gamma_y < 12(1-\nu^2)$, $\alpha \geq 1 \wedge \gamma_y < 12(1-\nu^2)$, $\alpha < 1 \wedge \gamma_y \geq 12(1-\nu^2)$ and $\alpha \geq 1 \wedge \gamma_y \geq 12(1-\nu^2)$. The choice of having two ranges split for $\gamma_y = 12(1-\nu^2)$ ($\approx$10.92 for steel) comes from the analysis made to Fig. 10, where the buckling mode changes for values around 10.

$$k_\tau = c_1 + \frac{c_2}{\alpha} + \frac{c_3}{\alpha^2} + \frac{c_4}{\sqrt[3]{\gamma_y}} + \frac{c_5}{\sqrt[3]{\gamma_z}} + \frac{c_6}{\sqrt[3]{\phi_x}} + c_7 \cdot \alpha^{c_8} \cdot {\gamma_y}^{c_9} \cdot {\gamma_z}^{c_{10}} \tag{19}$$

The c_i parameters were obtained for each subset employing the *FindFit* function implemented in Mathematica [34], yielding Eqs. (20) and (21), respectively, for open and closed cross-section stiffeners over the compression diagonal. To match the proposed model with existing formulae for unstiffened panels, c_1 and c_2 were fixed for $\alpha < 1 \wedge \gamma_y < 12(1-\nu^2)$ ($c_1 = 4$ and $c_2 = 5.34$) and for $\alpha \geq 1 \wedge \gamma_y < 12(1-\nu^2)$ ($c_1 = 5.34$ and $c_2 = 4$ for $\alpha \geq 1$). Additionally, in what concerns open stiffeners over the compression diagonal, c_{10} was set to zero translating the negligible influence of ϕ_x in the results.

$$k_\tau = \begin{cases} 4.00 + \dfrac{5.34}{\alpha^2} + \dfrac{11.50}{\sqrt[3]{\gamma_y}} + 5.23 \cdot \dfrac{\gamma_y^{0.404} \cdot \gamma_z^{0.038}}{\alpha^{1.371}} \\ \quad for\ 0.5 < \alpha \leq 1 \wedge \gamma_y \leq 12\left(1-\nu^2\right) \\ 5.34 + \dfrac{4.00}{\alpha^2} + \dfrac{4.07}{\sqrt[3]{\gamma_y}} + 6.15 \cdot \dfrac{\gamma_y^{0.428} \cdot \gamma_z^{0.020}}{\alpha^{1.434}} \\ \quad for\ 1 < \alpha \leq 2 \wedge \gamma_y \leq 12\left(1-\nu^2\right) \\ 18.35 + \dfrac{5.67}{\alpha} + \dfrac{3.35}{\alpha^2} - \dfrac{17.96}{\sqrt[3]{\gamma_y}} + 10.16 \cdot \dfrac{\gamma_y^{0.026} \cdot \gamma_z^{0.076}}{\alpha^{1.788}} \\ \quad for\ 0.5 < \alpha \leq 1 \wedge \gamma_y > 12\left(1-\nu^2\right) \\ 12.03 + \dfrac{9.96}{\alpha} + \dfrac{11.45}{\alpha^2} - \dfrac{14.29}{\sqrt[3]{\gamma_y}} + 6.92 \cdot \dfrac{\gamma_z^{0.375}}{\alpha^{1.632} \cdot \gamma_y^{0.036}} \\ \quad for\ 0.5 < \alpha \leq 1 \wedge \gamma_y > 12\left(1-\nu^2\right) \end{cases} \tag{20}$$

$$k_\tau = \begin{cases} 4.00 + \dfrac{5.34}{\alpha^2} + \dfrac{5.03}{\sqrt[3]{\gamma_y}} + \dfrac{1.46}{\sqrt[3]{\phi_x}} + 5.95 \cdot \dfrac{\gamma_y^{0.344} \cdot \gamma_z^{0.086}}{\alpha^{1.557}} \\ \quad for\ 0.5 < \alpha \leq 1 \wedge \gamma_y \leq 12\left(1-\nu^2\right) \\ 5.34 + \dfrac{4.00}{\alpha^2} + \dfrac{3.85}{\sqrt[3]{\gamma_y}} - \dfrac{1.25}{\sqrt[3]{\phi_x}} + 6.81 \cdot \dfrac{\gamma_y^{0.395} \cdot \gamma_z^{0.011}}{\alpha^{1.083}} \\ \quad for\ 1 < \alpha \leq 2 \wedge \gamma_y \leq 12\left(1-\nu^2\right) \\ 24.49 + \dfrac{13.62}{\alpha^2} - \dfrac{17.01}{\sqrt[3]{\gamma_y}} + \dfrac{56.50}{\sqrt[3]{\gamma_z}} - \dfrac{64.40}{\sqrt[3]{\phi_x}} + 2.19 \cdot \dfrac{\gamma_z^{0.641}}{\alpha^{1.942} \cdot \gamma_y^{0.211}} \\ \quad for\ 0.5 < \alpha \leq 1 \wedge \gamma_y > 12\left(1-\nu^2\right) \\ 17.34 + \dfrac{16.48}{\alpha^2} - \dfrac{10.70}{\sqrt[3]{\gamma_y}} + \dfrac{25.62}{\sqrt[3]{\gamma_z}} - \dfrac{29.04}{\sqrt[3]{\phi_x}} + 2.95 \cdot \dfrac{\gamma_z^{0.563}}{\alpha^{1.578} \cdot \gamma_y^{0.170}} \\ \quad for\ 0.5 < \alpha \leq 1 \wedge \gamma_y > 12\left(1-\nu^2\right) \end{cases} \tag{21}$$

The statistical characterisation of the fits made by Eqs. (20) and (21) is made by assessing the value of R-square, mean, coefficient of variation and maximum absolute error, all given in Table 3. It is possible to conclude that both fits present an excellent level of agreement with numerical results.

6. Conclusions

This paper provides a thorough investigation of the elastic shear buckling behaviour of simply supported diagonally stiffened plates. The main goals were to define the buckling behaviour of diagonally stiffened plates and propose reliable formulae to predict the elastic critical stress. This investigation comprised more than 36 535 linear buckling analyses divided into two types of FE models.

The first set of models uses shell FE to model the plate and beam FE to model the diagonal stiffener, which is symmetrically placed in respect to the plate's middle plane. The main conclusion of the numerical results is that the elastic buckling behaviour strongly depends on the mechanical characteristics of the stiffener. Specifically, it is worth highlighting the following:

- Placing the stiffener over the compression diagonal is more effective than placing it over the tension diagonal: increments in the elastic critical stress over 500% for open stiffeners over the compression diagonal against increments around 50% for open stiffeners over the tension diagonal.
- Varying the stiffener's weak axis rigidity has a strong impact on the elastic critical stress when it is over the compression diagonal (increment around 80%);
- Varying the stiffener's torsional rigidity and its strong and weak axis rigidity impact elastic critical stress substantially, whether the stiffener is over the compression or tension diagonal (increments equal to 530% and 130%, respectively). The isolated effect of varying the stiffener's torsional rigidity alone is an increment of 16%–17% when placed over the compression diagonal and 79%–89% when placed over the tension diagonal.

The second set of analyses uses shell FE to model the stiffener placed over the compression diagonal at one side of the plate (unsymmetrical layout). The c_i parameters in Eq. (19) are fitted from a nonlinear regression analysis using the numerical results (more than 18 600). Finally, two models for the elastic shear buckling coefficients were proposed: Eq. (20) for open stiffeners and Eq. (21) for closed cross-section stiffeners. The statistical parameters were calculated, showing that the proposed formulae represent reliable and accurate models to predict diagonal stiffened plates' elastic shear buckling coefficients.

Finally, this paper is intended to be the first out of three that the authors hope will contribute to the design of diagonally stiffened plates. The papers which will follow will be concerned with experimental results and numerical calibration of models and with the calibration of the formulae to compute the ultimate resistance. The present paper is the first step to the design of diagonally stiffened plates, where formulae to compute the elastic critical shear stress is provided and thus allowing to compute the slenderness of the stiffened plate, a parameter required in most of the currently available design procedures

CRediT authorship contribution statement

J.P. Martins: Conception and design of study, Analysis and/or interpretation of data, Writing – original draft, Writing – review &

editing. **H.S. Cardoso:** Conception and design of study, Acquisition of data, Writing – original draft.

Declaration of competing interest

The authors declare that they have no known competing financial interests or personal relationships that could have appeared to influence the work reported in this paper.

Acknowledgements

Financial support from the Portuguese Ministry of Science, Technology and Higher Education (Ministério da Ciência, Tecnologia e Ensino Superior) under Grant PTDC/ECI-EGC/31545/2017 is gratefully acknowledged. The work was also financed by FEDER funds through the Competitivity Factors Operational Programme - COMPETE and by national funds through FCT – Foundation for Science and Technology within the scope of the project POCI-01-0145-FEDER-007633 and through the Regional Operational Programme CENTRO2020 within the scope of the project CENTRO-01-0145-FEDER-000006. Approval of the version of the manuscript to be published: J.P. Martins and H.S. Cardoso.

References

[1] G.H. Bryan, On the stability of thin plates under thrusts in its own plane, with applications to the 'buckling of the sides of a ship, Proc. Lond. Math. Soc. 22 (1) (1981) 54–67.
[2] S. Timoshenko, Stability of rectangular plates with stiffeners, Mem. Inst. Eng. Ways Commun. 89 (23) (1915) (in Russian).
[3] F. Bleich, Buckling of Metal Structures, in: Engineering Societies Monographs, MacGraw-Hill, New York, 1952.
[4] I.T. Cook, K.C. Rockey, Shear buckling of rectangular plates with mixed boundary conditions, Aeronaut. Q. 14 (4) (1963) 349–355.
[5] P.S. Bulson, Stability of Flat Plates, American Elsevier, New York, 1970.
[6] H. Crate, H. Lo, Naca technical note (1589), 1948.
[7] T. Höglund, Shear buckling resistance of steel and aluminium plate girders, Thin-Walled Struct. 29 (1–4) (1997) 13–30.
[8] B. Johansson, R. Maquoi, G. Sedlacek, C. Müller, D. Beg, Commentary and Worked Examples to EN1993-1-5 Plated Structural Elements, Joint Research Centre, 2007.
[9] K. Klöppel, J. Scheer, Beulwerte Ausgesteifter Rechteckplatten, Wilhelm Ernst & Sohn, 1960, (in German).
[10] CEN, 2020. prEN1993-1-5:2020: Plated structural elements (ref: CEN/TC250/SC3-N3207), Brussels.
[11] B. Jáger, L. Dunai, Bending and shear buckling interaction behaviour of I-girders with longitudinally stiffened webs, J. Construct. Steel Res. 145 (2018) 504–517.
[12] L. Pavlovčič, A. Detzel, U. Kuhlmann, D. Beg, Shear resistance of longitudinally stiffened panels – part 1: tests and numerical analysis of imperfections, J. Construct. Steel Res. 63 (2007) 337–350.
[13] L. Pavlovčič, D. Beg, U. Kuhlmann, Shear resistance of longitudinally stiffened panels – part 2: numerical parametric study, J. Construct. Steel Res. 63 (2007) 351–364.
[14] U. Kuhlmann, B. Braun, A. Detzel, M. Feldmann, J. Naumes, M. Oppe, Y. Galéa, P.O. Martin, J. Raoul, L. Davaine, B. Johansson, M. Clarin, J. Gozzi, H. Degée, N. Boissonnade, J. Chica, F. Rey, Competitive Steel and Composite Bridges By Improved Steel Plated Structures (COMBRI), Final Report, RFS-CR-03018, European Commission - Research Fund for Coal and Steel, 2007.
[15] F. Sinur, D. Beg, Moment–shear interaction of stiffened plate girders – tests and numerical model verification, J. Construct. Steel Res. 85 (2013) 116–129.
[16] F. Sinur, D. Beg, Moment–shear interaction of stiffened plate girders – numerical study and reliability analysis, J. Construct. Steel Res. 85 (2013) 231–243.
[17] P. Dubas, E. Gehri, Structural Stability, Behaviour and Design of Steel Plated Structures, European Convention for Constructional Steelwork (ECCS), Publication no. 44, 1986.
[18] H.X. Yuan, X.W. Chen, M. Theofanous, T.Y. Cao, X.X. Du, Shear behaviour and design of diagonally stiffened stainless steel plate girders, J. Construct. Steel Res. 153 (2019) 588–602.
[19] H. Yonezawa, I. Miakami, M. Dogaki, H. Uno, Shear strength of plate girders with diagonally stiffened webs, Proc. Jpn. Soc. Civ. Eng. 1 (1978) 7–27, (in Japanese).
[20] J.D. Glassman, V. Boyceb, M.E.M. Garloc, Effectiveness of stiffeners on steel plate shear buckling at ambient and elevated temperatures, Eng. Struct. 181 (2019) 491–502.
[21] . Simulia, ABAQUS FEA (Version 6.17), Simulia Dassault Systèmes, 2017.
[22] P. Dubas, H. Tschampeer, Stabilite des ames soumises a une charge concentree et a une flexion globale, Constr. Metallique 27 (2) (1990) 25–39, (in French).
[23] C. Graciano, O. Lagerqvist, Critical buckling of longitudinally stiffened webs subjected to compressive edge loads, J. Construct. Steel Res. 59 (9) (2003) 1119–1146.
[24] N. Loaiza, C. Graciano, R. Chacón, E. Casanova, A comparative analysis of longitudinal stiffener cross-section for slender I-girders subjected to patch loading, Ce/Papers 1 (2–3) (2017) 4223–4229.
[25] N. Loaiza, C. Graciano, E. Casanova, Web slenderness for longitudinally stiffened I-girders subjected to patch loading, J. Construct. Steel Res. 162 (2019) 105737.
[26] N. Markovic, S. Kovacevic, Influence of patch load length on plate girders, part I experimental research, J. Construct. Steel Res. 157 (2019) 207–228.
[27] U.Beg.D. Kuhlmann, L. Davaine, B. Braun, Design of Plated Structures, ECCS Eurocode Design Manuals, Ernst & Sohn, 2010.
[28] A. Carretero, J.P. Lebet, Introduction des forces concentrées dans les poutres élancées, Constr. Metallique 1 (1998) 5–18, (in French).
[29] U. Kuhlmann, B. Braun, A. Detzel, M. Feldmann, J. Naumes, M. Oppe, Y. Galéa, P.-O. Martin, J. Raoul, L. Davaine, B. Johansson, M. Clarin, J. Gozzi, R. Maquoi, H. Degée, N. Boissonnade, J. Chica, F. Espiga, J. Grijalvo, F. Rey, G. Uria, F. Nüsse, F. Schröter, ComBri — Competitive Steel and Composite Bridges By Improved Steel Plated Structures, RFCS Project Report, Contract RFS-CR-03018, Brussels, 2008.
[30] L. Pavlovˇcič, A. Detzel, U. Kuhlmann, D. Beg, Shear resistance of longitudinally stiffened panels – part 1: tests and numerical analysis of imperfections, J. Construct. Steel Res. 63 (2007) 337–350.
[31] M. Seitz, Tragverhalten Längsversteifter Blechträger Unter Quergerichteter Krafteinleitung (Doctoral thesis), Universität Stuttgart, Mitteilung des Instituts für Konstruktion und Entwurf Nr. 2005–2, 2005, (in German).
[32] F. Sinur, D. Beg, Moment–shear interaction of stiffened plate girders – tests and numerical model verification, J. Construct. Steel Res. 85 (2013) 116–129.
[33] A. Biscaya, J.O. Pedro, U. Kuhlmann, Experimental behaviour of longitudinally stiffened steel plate girders under combined bending, shear and compression, Eng. Struct. 238 (2021) 112139.
[34] Wolfram Research, Inc., Mathematica, Version 12.0.